

Corrections to Fixed Analyzer Measurements of Polarization Mode Dispersion

P. A. Williams and C. M. Wang

Abstract - We report computer simulation results of polarization mode dispersion (PMD) measurements using the fixed analyzer technique. We find a new value for the polarization mode coupling factor of 0.805 (a 2% difference with the old value of 0.824). Systematic biases due to sampling density and extrema thresholding are quantified (6-12% for typical measurement conditions), and a simple correction algorithm is presented which removes the effects of these biases within $\pm 1.7\%$.

Index Terms - Fixed analyzer, k factor, mode coupling, peak counting, PMD, polarization mode dispersion, sampling density, wavelength scanning.

I. INTRODUCTION

Among the methods of polarization mode dispersion (PMD) measurement, the fixed analyzer technique is perhaps the simplest to use. Over its lifetime, some empirical techniques for noise reduction and sampling parameters have been generally adopted. In this paper, we examine in detail the characteristics and associated uncertainties of extremum thresholding and sampling density.

In its simplest configuration, a fixed analyzer measurement can be made using the set up of Fig. 1: a spectrally broad source (or alternatively a tunable laser), a pair of polarizers with the specimen in between, and an optical spectrum analyzer (or simple detector in the case of the tunable laser). For a specimen with a high degree of polarization mode coupling, the spectral intensity $T(\omega)$ where ω is optical frequency, at the detector will have a quasi-random output resembling Fig. 2. Poole and Favin have shown that the PMD of the specimen is proportional to the number of extrema or the number of mean-value crossings in $T(\omega)$ [1]. In extremum counting, the accuracy of the measurement relies on correct wavelength measurement and identification of extrema. Extremum identification is altered by sampling the curve improperly and by the presence of noise in the system. We discuss the effects of these two error sources below.

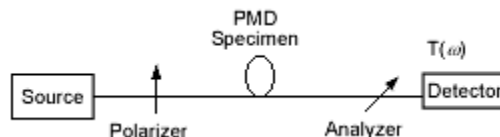


Fig. 1 Generic fixed analyzer PMD measurement apparatus.

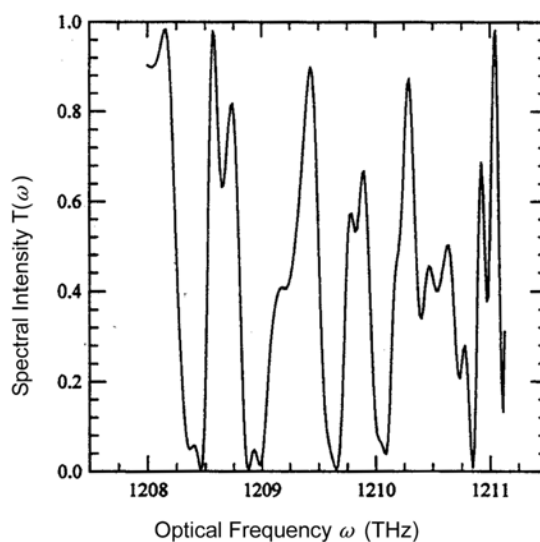


Fig. 2 Typical transmission spectrum for fixed analyzer PMD measurement.

II. SAMPLING DENSITY

For long fibers, Poole and Favin related the expected value of PMD $\langle \Delta \tau \rangle$ to the expected value of the number of mean-value crossings N_m .

$$\langle \Delta \tau \rangle = 4 \frac{\langle N_m \rangle}{\Delta \omega} \quad (1)$$

and to the expected value of the number of extrema N_e

$$\langle \Delta \tau \rangle = 0.824\pi \frac{\langle N_e \rangle}{\Delta \omega} \quad (2)$$

where $\Delta \omega$ is the width of the frequency window over which the measurement is taken. The factor 4 in (1)

was obtained analytically, while the factor 0.824 in (2) was obtained through Monte Carlo simulation [1].

In practice, measured values of N_m and N_e are used in place of $\langle N_m \rangle$ and $\langle N_e \rangle$ to estimate the PMD $\langle \Delta\tau \rangle$. Values of N_m and N_e in general depend on $\langle \Delta\tau \rangle$, $\Delta\omega$, and the sampling density $\eta = n_f / \langle \Delta\tau \rangle \Delta\omega$ (a unitless quantity where n_f is the number of points used to sample $T(\omega)$). Under regular conditions, N_m and N_e depend on $\langle \Delta\tau \rangle$ and $\Delta\omega$ only through their product $\langle \Delta\tau \rangle \Delta\omega$. That is, the smaller the PMD, the larger the spectral width required to estimate the PMD with the same precision. Since $T(\omega)$ is everywhere differentiable and continuous on ω , the number of discrete frequency measurements made will affect the outcome of N_m and N_e . In fact, N_m and N_e are nondecreasing functions of η . This means that if η is not sufficiently large, (1) and (2) will produce PMD estimates which are biased toward smaller values.

To study the effects of sampling density, we performed extremum counting and mean-value crossing measurements on $T(\omega)$ data from computer-simulated fixed analyzer measurements. Our simulation was much like that of Poole and Favin [1]. We simulated the fiber as a stack of 2700 waveplates with their optic axes randomly oriented. The differential group delay (DGD) $\Delta\tau_i$ between the fast and slow axes of each waveplate was randomly selected from a uniform distribution between 0 and $\Delta\tau_{\max} = 0.8556$ ps. This random DGD is different from that of Poole and Favin where the waveplates all had the same DGD. We used the Jones calculus to calculate the transmission spectrum $T(\omega)$ over the spectral window $\Delta\omega$ for propagation of light through the waveplate stack situated between a pair of polarizers. A full data set consisted of $T(\omega)$ data for 10 000 simulated fibers. A more detailed description of our simulation is given in Appendix A.

Let $\tilde{N}_m(\eta)$ and $\tilde{N}_e(\eta)$ be the means of N_m and N_e of the 10 000 simulated fibers measured with sampling density η . Fig. 3 plots $\tilde{N}_m(\eta)$ and $\tilde{N}_e(\eta)$ versus η . It clearly shows that $\tilde{N}_m(\eta)$ and $\tilde{N}_e(\eta)$ approach asymptotic limits as η becomes large. Since $\tilde{N}_m(\eta)$ and $\tilde{N}_e(\eta)$ are based on 10 000 fibers, they are very good estimates of $\langle N_m \rangle$ and $\langle N_e \rangle$ and we obtain the mode coupling factors used in (1) and (2) as a function of η . That is, we obtain

$$k_1(\eta) = \frac{\langle \Delta\tau \rangle \Delta\omega}{\tilde{N}_m(\eta)} \quad (3)$$

and

$$k_2(\eta) = \frac{\langle \Delta\tau \rangle \Delta\omega}{\pi \tilde{N}_e(\eta)} \quad (4)$$

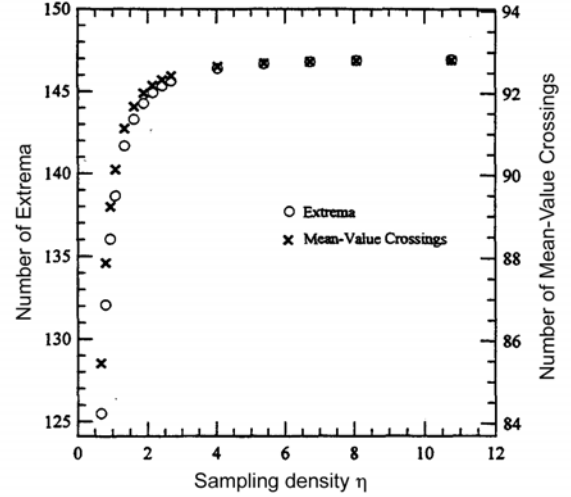


Fig. 3 Asymptotic behavior of measured number of extremum and mean-value crossings as a function of sampling density.

Table I

Results of PMD Measurements Made Using $k_2 = 0.805$ and 0.824 for simulations with various $\langle \Delta\tau \rangle$ (True PMD) and $\langle \Delta\omega \rangle$ values (all sampling densities were fixed at $\eta = 7$)

$\langle \Delta\tau \rangle$ (ps)	$\Delta\omega$ (ps^{-1})	n_f	PMD Estimate k=0.805, (ps)	PMD Estimate k=0.805, (ps)	standard error
10	5π	1100	9.97	10.21	0.029
40	5π	4400	40.05	41.00	0.058
23.65	3π	1560	23.62	24.17	0.058
23.65	7π	3640	23.61	24.17	0.038

A. Corrected Mode-Coupling Factor

Using (A4) to generate $\langle \Delta\tau \rangle$, we are able to calculate k_1 and k_2 . Fig. 4 plots our calculated values of k_1 and k_2 as functions of η and shows that k_1 converges to 4.00 ± 0.0037 (the predicted limit) as η becomes large. However, k_2 converges to 0.805 ± 0.0005 , not the predicted factor 0.824. The agreement of our k_1 with the closed-form prediction of 4 verifies the integrity of our simulation and lends support to our k_2 value. In order to further verify k_2 , we performed several more simulations (of 1000 fibers each) for various values of PMD $\langle \Delta\tau \rangle$ and frequency window $\Delta\omega$, holding the sampling density η constant at approximately seven. Table I shows the simulation

results of PMD measurements using $k_2 = 0.805$ and $k_2 = 0.824$. The estimated PMD using 0.805 always agrees with the theoretical PMD $\langle \Delta\tau \rangle$ within $\pm 2u$ ($u =$ standard uncertainty [2]), whereas the PMD estimates using 0.824 are not even within a $\pm 3u$ band of the true PMD. We further verified the simulation by using a small-value PMD as well. 10 000 fibers were simulated with $\langle \Delta\tau \rangle = 0.5$ ps, and $\eta \approx 11$ ($n_f = 400$). Using $k_2 = 0.805$, we measured a PMD of 0.4981 ps; $k_2 = 0.824$ gave a PMD of 0.5098 ps and $u = 0.000952$ ps for both measurements.

As for experimental proof that $k_2 = 0.805$, the large inherent uncertainties in PMD measurements [(5) and (6)] make a 2% discrepancy difficult to verify. Though several experimental comparisons have been made [3]-[5], none have sufficient numbers of statistically independent measurements on highly mode-coupled fibers to verify k_2 within 2%. In fact, in order to experimentally measure k_2 within, say, 1%, using a 100 nm spectral-width source on fibers with a nominal PMD of 1 ps would require at least 158 statistically independent measurements.

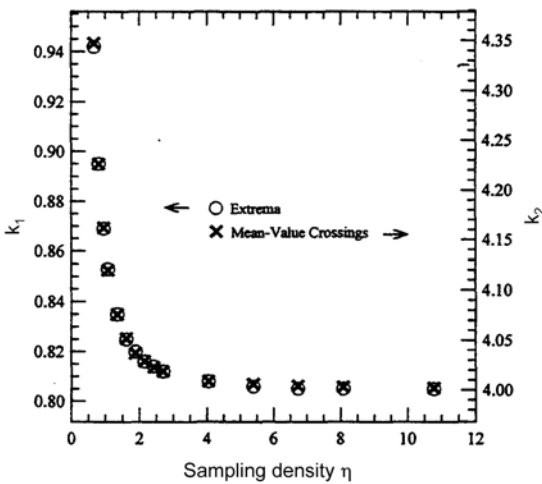


Fig. 4 Calculated mode coupling constants versus sampling density.

In trying to identify the source of the 2% disagreement between our value of k_2 and that of Poole and Favin, we have three possible culprits. The most likely candidate would be if Poole and Favin had an insufficient sampling density. Fig. 4 demonstrates that using the slightly low value of $\eta = 1.6$ would be sufficient to give the 2% bias to k_2 . However, this hypothesis cannot be verified as the Poole and Favin paper contains a typographical error in reporting the sampling density. A part of this discrepancy might also be explained as being due to the use of waveplates of fixed versus random DGD.

We demonstrated this by performing a simulation of 10 000 fibers using fixed DGD waveplates and the same parameters as Poole and Favin used. Plotting measured values of k_1 and k_2 as a function of η , similarly to Fig. 4, we found that k_1 converged to 0.404, and k_2 to 0.809. Therefore, their numbers might be biased slightly due to the use of the fixed DGD plates. A third source of uncertainty in Poole and Favin's value could have come in their estimate of the expectation value of $T''(\omega)$, which required the extrapolation to $\omega = 0$ of a fourth-order polynomial fit to the simulated data. In light of these possible error sources, the 2% discrepancy is explainable as simply a slight improvement in the uncertainty of our simulation over that of Poole and Favin.

B. Optimum Sampling Density

The fact that k_1 and k_2 are functions of sampling density brings to mind the question of what is the optimum sampling density. Clearly, sampling with too few points will yield fewer extrema (or mean crossings) underestimating the PMD. On the other hand, sampling too densely is redundant, magnifies the effect of noise in the system and extends the measurement time. If the asymptotic values of $k_1 = 4$ and $k_2 = 0.805$ are used at insufficient sampling density, we find an inflated uncertainty associated with the PMD estimate.

Fig. 5 displays the standard uncertainty of the PMD estimate as a function of η (based on 10 000 simulated fibers). For $\eta > 2$, the uncertainty is

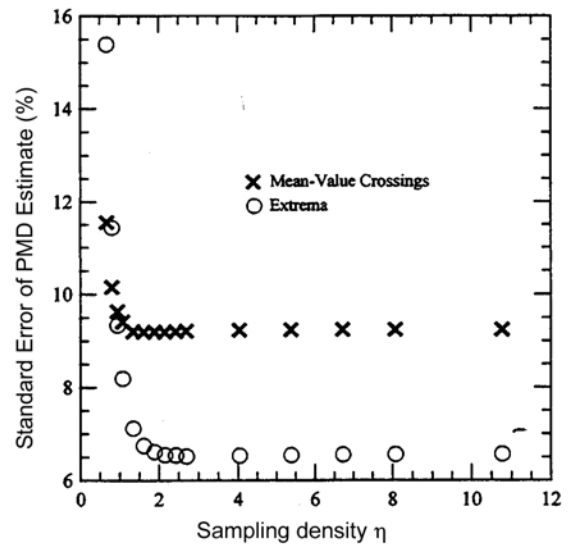


Fig. 5 Standard error of extremum counting and mean-value crossing measurements as a function of sampling density.

dominated by the inherent random statistical

uncertainty of the measurements [1]

$$\left(\frac{\sigma^2}{\langle \Delta\tau \rangle^2} \right)_{\text{MeanLevel}} \approx 0.44 \frac{2\pi}{\langle \Delta\tau \rangle \Delta\omega} \quad (5)$$

$$\left(\frac{\sigma^2}{\langle \Delta\tau \rangle^2} \right)_{\text{extrema}} \approx 0.21 \frac{2\pi}{\langle \Delta\tau \rangle \Delta\omega} \quad (6)$$

If $\eta < 2$, these errors will be dominated by a systematic bias due to insufficient sampling. Therefore, in order to minimize uncertainty, at least $2\langle \Delta\tau \rangle \Delta\omega$ frequency points should be sampled. As an example of the requirement this imposes, Table II demonstrates the wavelength resolution $\Delta\lambda_{\text{max}}$ required to achieve the $\eta \geq 2$ condition for various values of PMD (at a center wavelength of 1550 nm). In the next section, we will discuss a normalization technique which reduces the errors associated with improper sampling densities.

Table II
Maximum Wavelength Step Allowed by $\eta \geq 2$ requirement for various PMD Values

PMD (ps)	0.1	0.5	1	2	5	10
$\Delta\lambda_{\text{max}}$ (nm)	6.4	1.3	0.64	0.32	0.13	0.064

III. NOISE EFFECTS

In extremum counting, the PMD estimate is proportional to the number of extrema and so is very sensitive to the presence of noise in the system. A popular noise reduction method is to count as extrema only those maximum and minimum points which surpass some threshold height or depth ϵ . However, thresholding has the often overlooked problem of also eliminating some "real" peaks from consideration. Here, we quantify the effects of thresholding on the measured PMD.

A. Extremum Thresholding

Before discussing results, it is necessary to define what is meant by extremum thresholding. The simplest approach to extremum thresholding is to determine the height of a peak and the adjacent valley as the absolute difference between their $T(\omega)$ levels. However, this technique does not work well for noisy data where the density of noise peaks is comparable to, or larger than, the density of real peaks. Consider the example of Fig. 6. The $T(\omega)$ curve shown represents wavelength scanning data with about 5% intensity noise. Using this technique with, say, an

8% threshold would eliminate the broad valley V (which is a real feature) from the extremum list. We use here a more robust definition of peak height where "extremum pairs" are identified as being the closest peak and valley whose extent $T(\omega_{\text{peak}}) - T(\omega_{\text{valley}})$ is greater than ϵ . A detailed description of the algorithm is given in Appendix B.

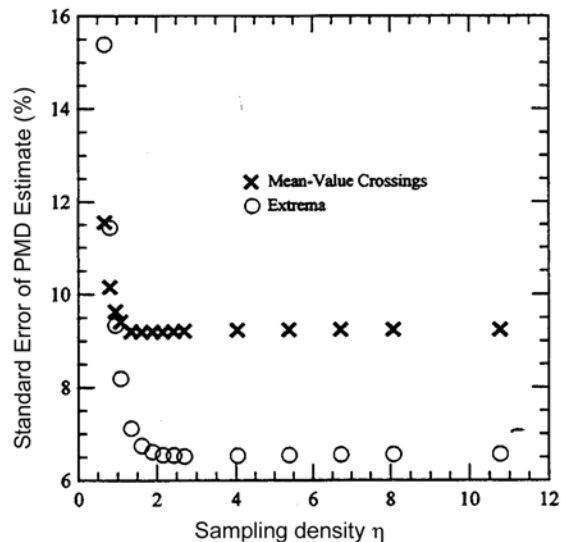


Fig. 6 Standard error of extremum counting and mean-value crossing measurements as a function of sampling density.

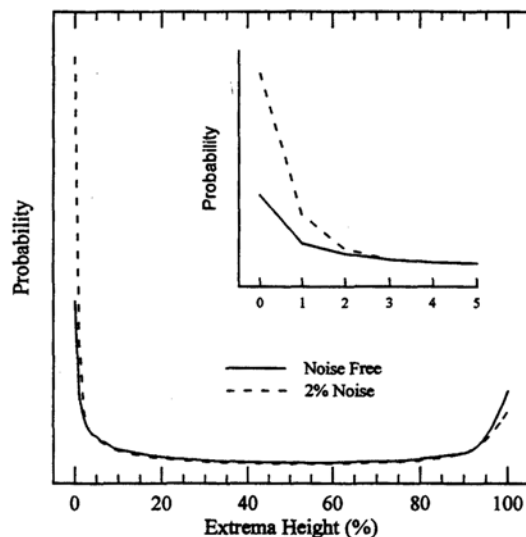


Fig. 7 Probability distribution of peak heights in the transmission spectrum from a fixed analyzer measurement. The inset shows the detail at small values.

Using this extremum pair algorithm, we evaluated 10 000 simulated $T(\omega)$ data sets to which 0, 1, and 2% random amplitude noise was added. The noise was from a triangular distribution with, for example, 1 %

referring to the maximum noise amplitude with respect to the maximum extent of $T(\omega)$. In Fig. 7, we show the sample distribution of peak heights for the noise free and 2% noise cases (measured at sampling density $\eta = 2.7$). The most surprising feature is the large number of small peaks in the noise free data. As expected, the 2% noise curve shows that noise significantly increases the number of small peaks, and thresholding is necessary in order to avoid biases toward larger PMD. So, in practice, noisy data will give too large a PMD value before thresholding and too small a PMD value afterward.

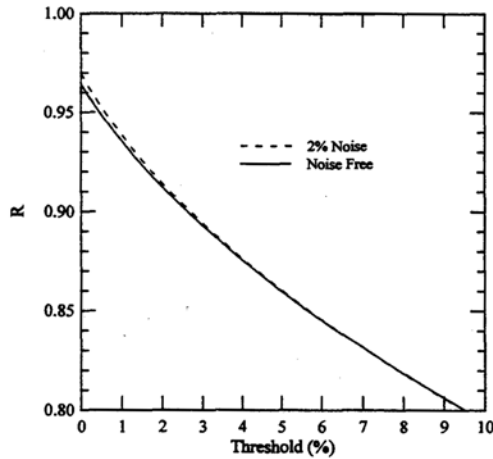


Fig. 8 Fractional PMD ($R = \text{Measured PMD}/\text{True PMD}$) as a function of noise threshold for undersampled ($\eta = 1.35$) noise free and 2% noise data.

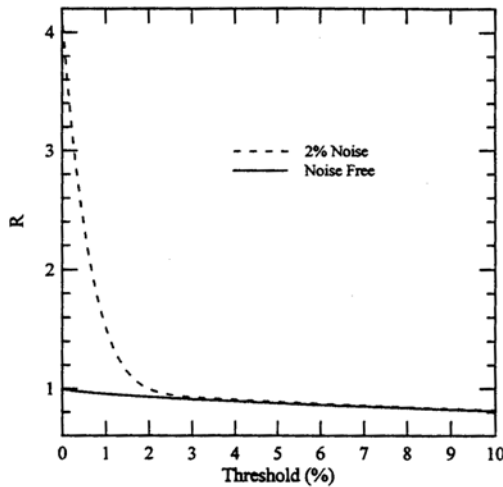


Fig. 9 Fractional PMD ($R = \text{measured PMD}/\text{truePMD}$) as a function of noise threshold for oversampled ($\eta = 10.77$) noise free and 2% noise data.

Figs. 8 and 9 show the effects of sampling density, noise and threshold on the measured PMD. Fig. 8 plots the ratio $R = \text{measured PMD}/\text{true PMD}$ versus percent threshold level for undersampled data ($\eta =$

1.35, $n_f = 500$) with 0 and 2% noise.

Fig. 9 is the same format for oversampled data ($\eta = 10.77$, $n_f = 4000$). Comparing the two shows that oversampling dramatically increases the bias to measured PMD when thresholds are below the actual noise level, whereas in undersampled data, there is little effect at all due to noise. For the noise levels tested, thresholds of $\epsilon > 4\%$ yield measured PMD values which are independent of noise level.

B. Compensation for Noise and Sampling Density

The best approach to measurements in the presence of noise is to threshold well above the noise and then correct for the systematic bias due to the high threshold. To study the correction factor, we simulated fibers with $\langle \Delta\tau \rangle \Delta\omega$ values of 36.4, 58.2, 145.6, and 371.5 and noise levels of 0, 1, and 2% (1000 fibers for each of the 12 combinations). Then, for each of these fibers, $T(\omega)$ was measured using sampling densities ranging from 1 to 10 in 0.5 increments. For each parameter combination, the ratio

$$R = \frac{\text{MeasuredPMD}(\epsilon = 20\%)}{\text{TruePMD}} \quad (7)$$

was calculated. As mentioned, R is relatively independent of noise level. The dependence of R on $\langle \Delta\tau \rangle \Delta\omega$, η , and noise level is illustrated in Fig. 10.

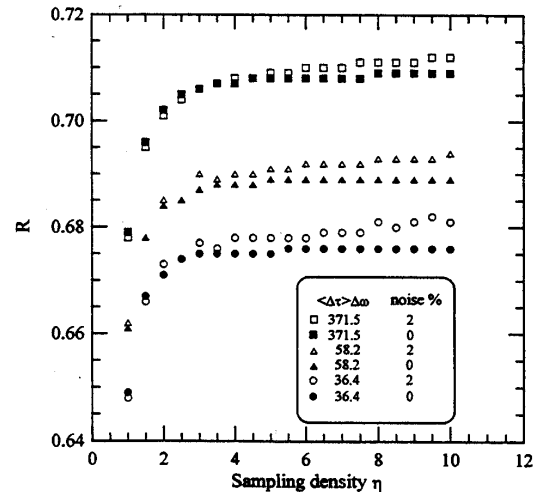


Fig. 10 Correction factor $R = \text{measured PMD} (\epsilon = 20\%)/\text{true PMD}$ versus sampling density for various values of $\langle \Delta\tau \rangle \Delta\omega$ with and without 2% noise.

The weak dependence on these parameters suggests a

simple first-order correction factor using a midpoint value of $R_{\text{avg}} = 0.69$. Measuring PMD using a 20% extremum threshold and then dividing by 0.69 will give a corrected PMD whose $2u$ systematic uncertainty ($\sim 95\%$ confidence interval) due to sampling density and noise is below $\pm 6.3\%$ (if measurement parameters are within the limits of $36 \leq \langle \Delta\tau \rangle \Delta\omega \leq 371$, $1.5 \leq 10$ and noise $\leq 2\%$).

If smaller systematic uncertainties are required, a two-step correction is recommended. First, the $\pm 6.3\%$ PMD estimate is obtained as just described. Then this value is used to calculate $\langle \Delta\tau \rangle \Delta\omega$ and η . A more accurate $R(\langle \Delta\tau \rangle \Delta\omega, \eta)$ can then be chosen from Table III. Then, the original 20% threshold measurement of PMD is divided by the new $R(\langle \Delta\tau \rangle \Delta\omega, \eta)$ to get a PMD estimate with systematic uncertainties below $\pm 1.7\%$ ($2u$). We suggest using a linear interpolation for values of $\langle \Delta\tau \rangle \Delta\omega$ which are in between those included in Table III. The values in this table represent those R which we calculated based on our extremum counting simulations with various values of $\langle \Delta\tau \rangle \Delta\omega$, and η .

Table III
R-Factor as a Function of Sampling Density and PMD-Bandwidth Product

η	$\langle \Delta\tau \rangle \Delta\omega$			
	36.4	58.2	145.6	371.5
1	0.648	0.661	0.677	0.679
1.5	0.667	0.678	0.694	0.696
2	0.672	0.685	0.700	0.702
2.5	0.673	0.685	0.701	0.704
3	0.675	0.688	0.704	0.706
3.5	0.676	0.688	0.704	0.707
4	0.677	0.689	0.705	0.707
4.5	0.677	0.689	0.705	0.707
5	0.676	0.690	0.705	0.708
5.5	0.677	0.689	0.705	0.708
6	0.677	0.690	0.706	0.709
6.5	0.677	0.690	0.706	0.709
7	0.678	0.690	0.706	0.709
7.5	0.678	0.690	0.706	0.709
8	0.679	0.690	0.706	0.709
8.5	0.678	0.691	0.706	0.709
9	0.678	0.690	0.707	0.709
9.5	0.679	0.691	0.707	0.709
10	0.678	0.691	0.706	0.710

For comparison, an uncorrected extremum counting

measurement on data with 1% noise, using a 2% extremum threshold causes a 6-12% systematic uncertainty as illustrated in Fig. 11. These corrections apply only to the systematic errors due to sampling density and noise. The well-known random uncertainties of (5) and (6) still exist.

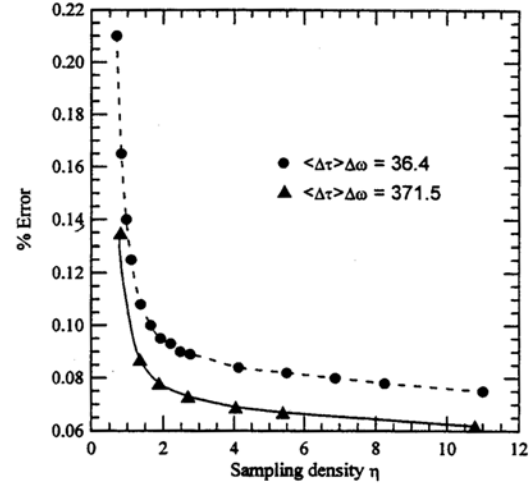


Fig. 11 Systematic errors in extremum counting measurements as a function of sampling density for 1% noise level, measured with a 2% threshold (for small and large values of $\langle \Delta\tau \rangle \Delta\omega$).

IV. CONCLUSION

We have demonstrated here that fixed analyzer

measurements made under typical conditions can be significantly biased. Figs. 3 and 11 show that $\sim 10\%$ biases are easily, achievable. Based on simulation results, we presented two correction techniques for these errors. The first is a correction factor R_{avg} , which can be applied to reduce systematic uncertainties to below $\pm 6.3\%$ over a broad range of measurement conditions. The second technique is a two step process which estimates measurement conditions and then a more appropriate factor is applied to reduce systematic uncertainties to below $\pm 1.7\%$. Finally, we found a 2% correction to the polarization mode coupling factor (commonly denoted k), changing its value to 0.805 from the previously accepted value of 0.824.

APPENDIX A COMPUTER SIMULATION

We simulated fiber PMD using the method of Poole and Favin [1] with a few changes. Random birefringence in the simulated fibers was modeled by

a cascade of waveplates with randomly oriented axes and random differential group delay (DGD) between the fast and slow axes. Let N be the number of waveplates and $\Delta\tau_i$ be the DGD for the i th waveplate. For large N , the expected value of the PMD $\langle\Delta\tau\rangle$ is given by [1]

$$\langle\Delta\tau\rangle = \sqrt{\frac{8}{3\pi} \sum_{i=1}^N \langle\Delta\tau_i^2\rangle} \tag{A1}$$

If $\Delta\tau_i$ are identically distributed, then

$$\sum_{i=1}^N \langle\Delta\tau_i^2\rangle = N(\langle\Delta\tau\rangle^2 + \sigma_{\Delta\tau}^2) \tag{A2}$$

where $\langle\Delta\tau\rangle$ and $\sigma_{\Delta\tau}^2$ are the expected value and variance of $\Delta\tau_i$. Poole and Favin used a fixed value of $\Delta\tau_i = \Delta\tau_0$ in their simulations. This assumption of constant DGD results in $\langle\Delta\tau\rangle^2 = \Delta\tau_0^2$ and $\sigma_{\Delta\tau}^2 = 0$, and reduces (A1) to

$$\langle\Delta\tau\rangle = \sqrt{\frac{8N}{3\pi}} \Delta\tau_0 \tag{A3}$$

If we allow $\Delta\tau_i$ to be uniformly distributed between 0 and $\Delta\tau_{\max}$, then $\langle\Delta\tau_i^2\rangle = \Delta\tau_{\max}^2 / 3$, and

$$\langle\Delta\tau\rangle = \sqrt{\frac{8N}{3\pi}} \frac{\Delta\tau_{\max}}{\sqrt{3}} \tag{A4}$$

To determine whether to use the fixed or random differential group delays in the simulation, we conducted a Monte Carlo study. For each fiber, we used $N = 2700$, $\Delta\tau_0 = 0.494$ ps for the fixed DGD case, and $\Delta\tau_{\max} = 0.494\sqrt{3} = 0.8556$ ps for the random case (to insure that the predicted PMD of the fiber is the same in the two cases). The transmission spectrum $T(\omega)$, starting at frequency $\omega_0 = 1.208 \times 10^{15} \text{ s}^{-1}$ with 1000 equally spaced frequencies over a total frequency window of $2.5 \times 2\pi \times 10^{12} \text{ s}^{-1}$, was obtained for both fixed and random DGD simulated fibers. We simulated 1000 fibers for each case.

Fig. 12 plots the mean of the 1000 simulated transmission spectra over the measured spectrum for fixed DGD. It shows two spikes over the frequency range. The spikes indicate the frequencies at which the retardance of each waveplate is a multiple of 2π . Our simulation was such that the "fiber" was situated between a pair of polarizers aligned parallel to each

other. So, at these $2\pi n$ retardance frequencies, the waveplate stack acts like an isotropic medium, and 100% of the light is transmitted through the analyzer. (Had we used crossed polarizers, these spikes would have been dips.) Since the theory yielding (1)-(6) relies on the assumption that the mean of the normalized transmission spectrum at any frequency is 0.5, the validity of the simulation samples based on fixed waveplate DGD is questionable. On the other hand, the mean of $T(\omega)$ for random DGD (Fig. 13) hovers around 0.5, indicating a good agreement between the simulated and theoretical means.

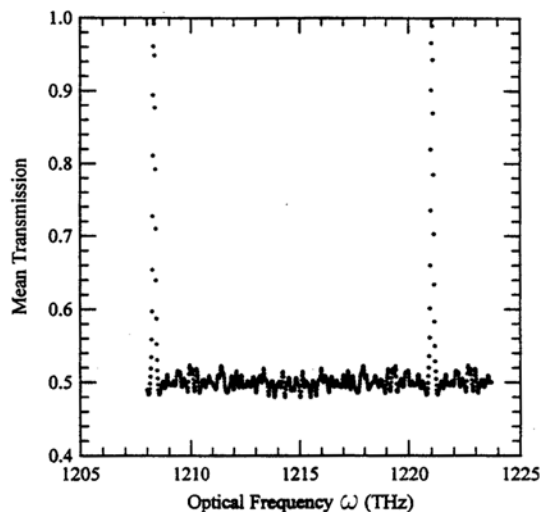


Fig. 12 Mean of $T(\omega)$ averaged over 1000 fibers as a function of optical frequency from simulation using fixed waveplate DGD.

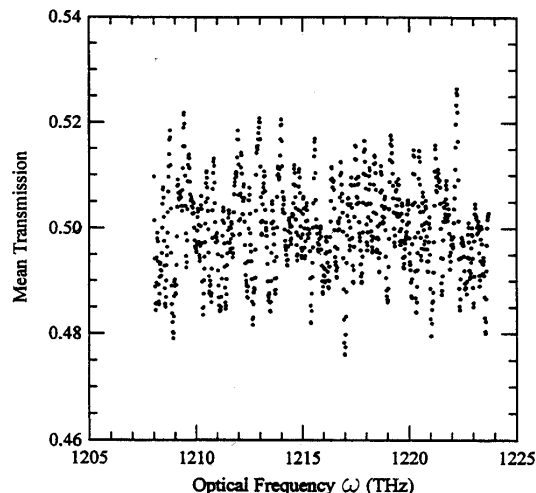


Fig. 13 Mean of $T(\omega)$ averaged over 1000 fibers as a function of optical frequency from simulation using random waveplate DGD.

We also examined the distribution of the number N_c

of extrema and the number N_m of mean-value crossings from the 1000 simulated fibers for both cases. Fig. 14 plots the smoothed probability density functions of N_e for the fixed (dotted line) and random (solid line) DGD. It shows that the means of the two probability density functions are about the same (144.6 for fixed, 145.6 for random) but the standard deviations of the distributions are different (14.51 for fixed, 9.43 for random). Similar results are also obtained for the distributions of N_m (Fig. 15), mean = 91.0 for fixed, 92.3 for random, standard deviation = 13.13 for fixed, 8.42 for random.

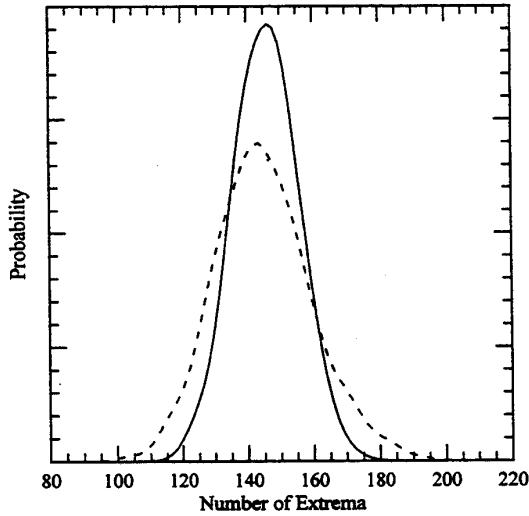


Fig. 14 Probability density function for extremum counts measured via simulations using random (solid line) and fixed (dashed line) waveplate DGD.

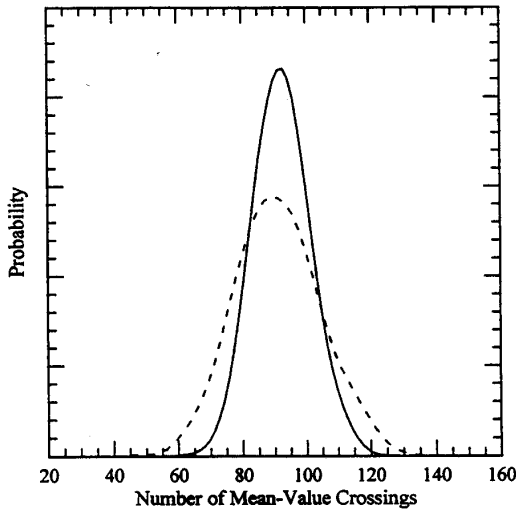


Fig. 15 Probability density function for mean-value crossing counts measured via simulations using random (solid line) and fixed (dashed line) waveplate DGD.

APPENDIX B (THRESHOLDING ALGORITHM)

Rejecting noise in an extremum counting routine is more subjective than it may seem. An effective algorithm must be able to reject the small extrema which are presumably due to noise while accepting the larger extrema. In this study we used the following algorithm to accept or reject extrema based on their height relative to the maximum extent of the spectral data $T(\omega)$. A pseudocode of the algorithm is given below. It is assumed that all of the extrema in $T(\omega)$ have been located and sequentially indexed using a three-point algorithm where $T(\omega_{i-1}) < T(\omega_i) > T(\omega_{i+1})$ indicates a peak, and $T(\omega_{i-1}) > T(\omega_i) < T(\omega_{i+1})$ a valley at ω_i .

```

right = index_of_global_max
candidate = right - 1 {test extremum to left of global
max}
left = candidate - 1
base = 1 {global max is a peak}
loop:
   $\delta_r = \text{abs}(T[\text{right}] - T[\text{candidate}])$ 
   $\delta_l = \text{abs}(T[\text{left}] - T[\text{candidate}])$ 
  if ( $\delta_r > \epsilon$  and  $\delta_l > \epsilon$ ) then
    {candidate is a good peak or valley}
    num_of_true_extrema = num_of_true_extrema + 1
    right = candidate
    candidate = right - 1
    left = candidate - 1
    base = - base
  else
    if ( $T[\text{left} - 1] * \text{base} \leq T[\text{candidate}] * \text{base}$ ) then
      candidate = left - 1
      left = candidate - 1
    else
      left = left - 2
    end if
  end if
end if

```

The base type 1 (-1) indicates that the current extremum is a peak (valley) and the target for peak thresholding with cutoff value s is the adjacent valley (peak). The algorithm is for scanning to the left of the global maximum. A similar algorithm for scanning to the right of the global maximum can be easily obtained. The complete listing of the Fortran program used can be obtained by contacting the authors.

ACKNOWLEDGEMENT

The authors would like to thank C. Poole for sharing his insight regarding the disagreement between the mode coupling factors.

REFERENCES

- [1] C. D. Poole and D. L. Favin, "Polarization-mode dispersion measurements based on transmission spectra through a polarizer," *J. Light wave Technol.*, vol. 12, pp. 917-929, 1994.
- [2] B. N. Taylor and C. E. Kuyatt, Eds., "Guidelines for evaluating and expressing the uncertainty of NIST measurement results," *Nat. Inst. Stand. Technol.*, Boulder, CO, Tech. Note 1297, 1994.
- [3] Y. Namiyama and J. Maeda, "Comparison of various polarization mode dispersion measurement methods in optical fibers," *Electron. Len.*, vol. 28, pp. 2265-2266, 1992.
- [4] Y. Namiyama and K. Nakajima, "Comparison of various polarization mode dispersion measurement methods in 1600 km EDFA system," *Electron. Len.*, vol. 30, pp. 1157-1158, 1994.
- [5] A. Galtarossa, G. Gianello, C. G. Smeda, and M. Schiano, "Infield comparison among polarization-mode-dispersion measurement techniques," *J. Lightwave Technol.*, vol. 14, pp. 42-49, 1996.

P. A. Williams was born in Flagstaff, AZ, in 1965. He received the B.S. degree in physics from Arizona State University, Tempe, in 1987 and the M.S. and Ph.D. degrees in physics from the University of Colorado, Boulder, in 1989 and 1993, respectively.

Since 1988, he has worked at the National Institute of Standards and Technology (NIST), Boulder, CO, in the field of optical metrology working with ferroelectric liquid crystals, polarization, and fiber optics.

C. M. Wang received the Ph.D. degree in statistics from Colorado State University, Fort Collins, in 1978.

He is a Mathematical Statistician in the Statistical Engineering Division, National Institute of Standards and Technology (MST), Boulder, CO. His research interests include interval estimation on variance components, statistical graphics and computing, and the application of statistical methods to physical sciences.